

using narrow-band, cw, tunable dye lasers or parametric oscillators. While Q values considerably smaller than that given by lifetime were obtained for ruby, much larger values are expected for suitable ion-host combinations. By restricting the direction of observation along the laser beam, the FLN technique is also expected to apply to gases in a manner similar to that described previously¹⁴ for a sequence of laser action and fluorescence. An advantage of FLN homogeneous linewidth observation over nonlinear absorption techniques¹⁵ is that many lines can be observed without tuning the laser. There are, of course, corresponding disadvantages, e.g., much spectral confusion when many overlapping lines are excited. The task of fine frequency control is now transferred to the detection system; thus, for example, we have the delightful prospect of observation of hyperfine, Zeeman, Stark, or stress spectra by heterodyne methods.

The author wishes to acknowledge with thanks the help of L. E. Erickson in constructing the equipment, the technical assistance of E. L. Dimock, and a useful encounter with G. R. Hanes at a critical point in the experiments.

¹R. H. Silsbee, in *Optical Properties of Solids*, edited by S. Nudelman and S. S. Mitra (Plenum, New York, 1969), p. 607.

²A. M. Stoneham, *Rev. Mod. Phys.* **41**, 82 (1969).

³A. Szabo, *Phys. Rev. Lett.* **25**, 924 (1970).

⁴M. Birnbaum, P. H. Wenzikowski, and C. L. Fincher, *Appl. Phys. Lett.* **16**, 436 (1970).

⁵N. Laurance, E. C. McIrvine, and J. Lambe, *J. Phys. Chem. Solids* **23**, 515 (1962).

⁶S. Geschwind, G. E. Devlin, R. L. Cohen, and S. R. Chinn, *Phys. Rev.* **137**, A1087 (1965).

⁷R. F. Wenzel, *Phys. Rev. B* **1**, 3109 (1970).

⁸T. Muramoto, Y. Fukuda, and T. Hashi, *J. Phys. Soc. Jap.* **26**, 1551 (1969).

⁹D. Grischkowsky and S. R. Hartmann, *Phys. Rev. B* **2**, 60 (1970).

¹⁰W. J. C. Grant and M. W. P. Strandberg, *Phys. Rev.* **135**, A727 (1964).

¹¹D. E. McCumber and M. D. Sturge, *J. Appl. Phys.* **34**, 1682 (1963).

¹²N. A. Kurnitt, I. D. Abella, and S. R. Hartmann, in *Physics of Quantum Electronics*, edited by P. L. Kelley, B. Lax, and P. E. Tannenwald (McGraw-Hill, New York, 1966), p. 267.

¹³There is however a dramatic apparent saturation effect when the passage of the laser beam through the crystal is viewed transversely. As the beam is focused down, the penetration increases from < 1 mm for a wide beam to over the entire sample length of 4 mm for a focused beam. The "saturation" occurs because of the net transfer of ions from the $(\pm \frac{1}{2})$ 4A_2 levels to the $(\pm \frac{3}{2})$ 4A_2 levels produced by optical-pumping effects similar to that in gases. The governing factors are the fluorescence lifetime (4 msec), the 4A_2 spin-lattice relaxation time (~ 200 msec at 4.2°K), and the spin-spin cross relaxation time in 4A_2 .

¹⁴W. G. Schweitzer, Jr., M. M. Birky, and J. A. White, *J. Opt. Soc. Amer.* **57**, 1226 (1967).

¹⁵G. R. Hanes and C. E. Dahlstrom, *Appl. Phys. Lett.* **14**, 362 (1969).

Band-Structure Effects in Metal-GaSb Tunnel Contacts Under Pressure*

P. Guétin and G. Schröder

Laboratoires d'Electronique et de Physique appliquée, 94 Limeil-Brevannes, France

(Received 30 April 1971)

Tunneling at 4.2°K from lead into degenerate n -type GaSb under hydrostatic pressure exhibits huge changes when conduction-band extrema cross each other. In the indirect-gap configuration, strong phonon-assisted structures show up together with a typical resistance kink related to the onset of a (000) tunneling path. The measured interband pressure coefficient is -9.6 meV/kbar. All results suggest that the band crossing occurs 3 kbar higher than expected.

Tunneling measurements in metal-GaSb contacts under hydrostatic pressure exhibit strong effects which are definitely due to the crossing of the Γ (000) and L (111) conduction-band extrema. Although band-structure effects in tunnel heterojunctions have previously been reported in the literature,¹⁻⁴ this work gives, to our knowledge, the first unambiguous quantitative

results concerning externally controlled band-structure effects in such junctions. Gallium antimonide is especially well suited for a systematic study of the tunnel mechanisms involved in direct- and indirect-gap semiconductors: The interband energy separation $E_L - E_\Gamma$ can be changed in both amplitude and sign by reasonably low pressure. GaSb is a direct-gap semiconductor⁵

at room pressure and the (111) valleys lie about 80 meV above the bottom (000) of the conduction band at 4.2°K. Hydrostatic pressure induces a shift of both conduction-band extrema toward higher energy with respect to the valence band. Since the rate of change of their energy difference, $(\partial/\partial P)(E_L - E_\Gamma)$, has been measured⁶ at -9.6 meV/kbar, the gap should become indirect around $P_0 = 8$ kbar. Roughly speaking the tunnel characteristics should present a GaAs-like behavior⁷ below P_0 and a Ge-like behavior at higher pressure. Above P_0 , two tunneling features characteristic of indirect-gap material are expected to occur: the appearance of zone-edge phonon-assisted tunneling⁸ and a resistance kink at reverse bias corresponding to the onset of tunneling into the higher valley.⁹ These effects should be detectable only if the effective masses satisfy $m_{\Gamma^*} \ll m_{L^*}$, a condition which is met by GaSb. This Letter confirms that these characteristics not only appear in n -GaAs above P_0 but constitute much stronger effects than in n -Ge.

Tunnel contacts were made by cleaving a (110) bar of n -GaSb:Te, doped at $4 \times 10^{18} \text{ cm}^{-3}$, in the stream of the evaporating metal (lead). During outgassing and evaporation the residual pressure was kept below 10^{-8} Torr. Measurements of first and second derivative versus the voltage V were carried out at 4.2°K up to 16 kbar (± 250 bar) at the Faculté des Sciences d'Orsay.¹⁰ Like Pb-GaAs contacts,¹¹ Pb-GaSb junctions have proved very reliable mechanically and undergo only minor irreversible changes under several pressure and temperature cycles. Changing the pressure actually requires warming up the transmitting fluid (isopentane) to room temperature. The quality of the tunnel contacts was checked by measuring at each pressure¹¹ the right superconducting density of states. No magnetic field could be applied and all the energies reported in the text have been corrected for the half-gap value Δ . Throughout this work $V > 0$ corresponds to electron injection from the semiconductor into the metal and conversely for $V < 0$. At zero bias, the background resistance $R(0)$ was about 0.1Ω at room pressure. Series resistances cannot be neglected; and, therefore, the corresponding curve on Fig. 1 is only indicative. Results below 9.6 kbar were purposely discarded for the same reason.

We first discuss the modification of the background resistance. $R(0)$ increases by a factor close to 10^5 when pressure is brought up from 0 to 15.7 kbar and its dependence on V is illus-

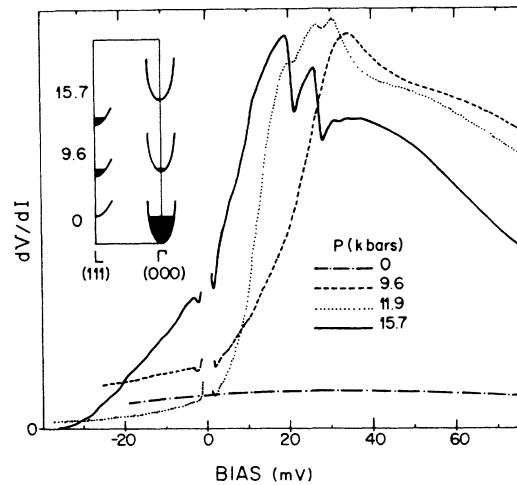


FIG. 1. dV/dI versus bias voltage for a Pb- n -GaSb tunnel contact at 4.2°K. The full vertical scale corresponds to 1.7, 35, 190, and 18 000 Ω for 0, 9.6, 11.9, and 15.7 kbar, respectively. The superconduction peak has been omitted for clarity. The insert sketches the GaSb conduction band and Fermi level.

trated in Fig. 1. The evolution of the shape of the differential resistance can be pictured along the following pattern. When pressure is increased from 0 to 10 kbar, approximately, the flat resistance curve steepens with a peaked maximum around 34 mV. This behavior can be qualitatively attributed to the progressive emptying of the (000) band and the corresponding filling of the (111) valleys. The steady decrease of the Fermi degeneracy $\mu_F(000)$ which is about 90 meV at $P = 0$ results in a widening of the depleted region. Other effects giving a resistance change include the increase of the barrier height¹¹ and the effective mass when pressure goes up. Around 10 kbar the conduction mechanism should involve both extrema, and no simple picture can be invoked in order to interpret the exact shape of the background.¹² Above 10 kbar the background shape stabilizes somewhat, and the bell-shaped curve essentially shifts towards the left of the figure as pressure goes up. When the (000) band becomes totally free of carriers, the Fermi level is only determined by the parameters of the (111) valleys. At the corresponding pressure P_1 , the change of tunneling mass results in a sharp resistance increase: Between 12 and 13 kbar we have observed that the resistance is multiplied by 10^2 . Above this *threshold pressure*, the (000) band no longer contributes to the forward tunneling process. The shape of the resistance background can be qualitatively inferred following Conley and Mahan's paper.⁷ In this

indirect-gap configuration, we estimate $\mu_F(111)$ and the "characteristic energy" $E_0(111)$ at 16 and 24 meV, respectively. Moreover, since the barrier height is much smaller than the (111) energy gap, the one-band model should represent a fair approximation to the actual dispersion relation in the barrier. Although $\mu_F(111)$ and $E_0(111)$ are of the same order of magnitude, one can expect that the position of the resistance maximum should be found close to $eV = \mu_F(111)$. Curves drawn around 10°K are not perturbed by appreciable inelastic tunneling and present indeed a resistance peak around $V = 18$ mV as expected.

The second interesting feature of the curves at high pressure can be pictured as a sharp resistance kink occurring at reverse bias, which

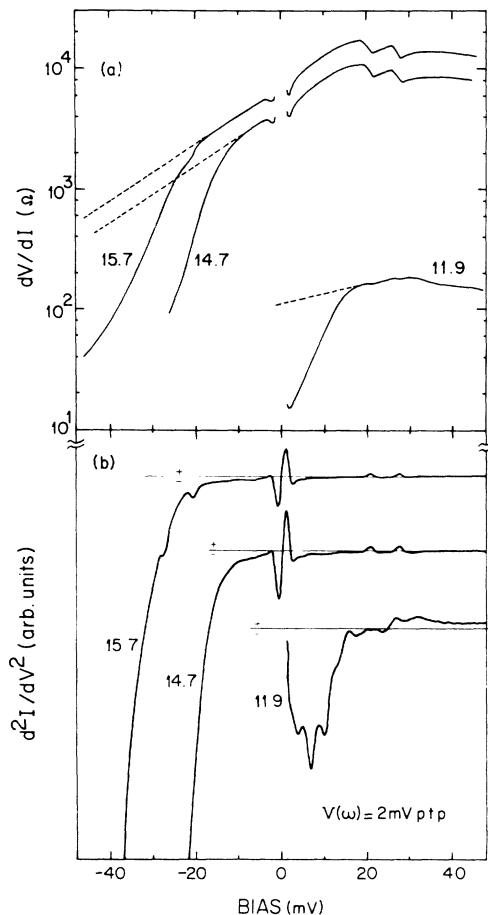


FIG. 2. (a) dV/dI on a logarithmic scale and (b) d^2I/dV^2 versus bias voltage for 11.9, 14.7, and 15.7 kbar showing the onset of tunneling in the (000) valley. Dashed lines represent estimated backgrounds. The superconducting zero-bias structure is only displayed in (b) but is smoothed out by the relatively large voltage modulation.

clearly appears on a semilogarithmic plot [Fig. 2(a)]. Figure 2(b) shows that the resistance kink manifests itself as a sharp, nearly vertical drop in d^2I/dV^2 : the higher the pressure, the more negative the corresponding threshold voltage. At 13 kbar the drop occurs at $V = 0$. This strongly suggests that the kink is due to the onset of tunneling into the higher band and is therefore closely related to Conley and Tiemann's results reported in the case of germanium.⁹ The threshold voltage is equal to $E_L - E_\Gamma + \mu_F(111)$, and its pressure dependence leads to an interband coefficient of -9.6 ± 1 meV/kbar, in close agreement with the above mentioned experimental determination.⁶ Below 13 kbar, however, a similar d^2I/dV^2 drop at $V > 0$ still occurs when the metal Fermi level aligns with the (000) band edge: Beyond this bias, no additional (000) carriers become available for tunneling.

The most spectacular feature of Fig. 1 consists obviously in the appearance of sharp, descending resistance steps around 20 and 25 mV. Their amplitude is very strong for $V > 0$ and weaker for $V < 0$ where they are buried in the dramatic resistance drop. Figure 2(b) shows that they are even in conductance. They can be best studied on a magnified second-derivative plot. Figure 3 compares curves drawn at 14.7 kbar and at room pressure.¹³ At $P = 0$ we mainly see two descending peaks which reflect the TA and LA phonon anomalies of the superconducting density of states. At 14.7 kbar, four definite extra structures have shown up. Starting from $V = 0$ the first one is found at 5.3 mV ($\Delta R/R = 7\%$) and

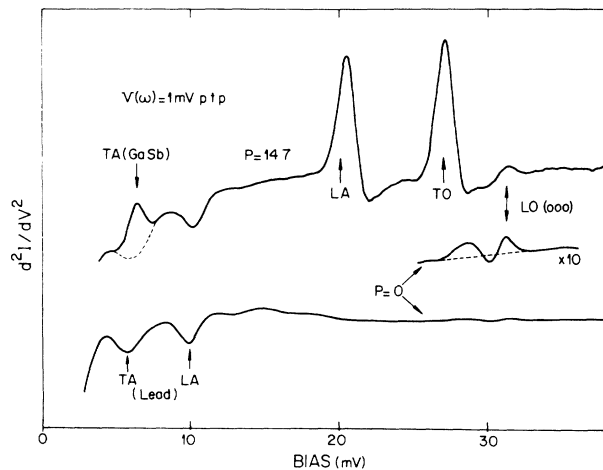


FIG. 3. d^2I/dV^2 versus forward voltage for $P = 0$ and 14.7 kbar showing the inelastic structures and the phonon indexation. Dashed lines represent estimated backgrounds.

mixes with the lead TA phonon structure. The next two at 19.4 and 26 mV have similar amplitudes (22–24%) and present noticeable undershoots partially due to the reflection of the superconducting density of states on their high-energy side. Symmetry strongly suggests that the first three structures are due to zone-boundary phonon-assisted tunneling which involves a transition from an L valley to the metal through an evanescent state of the Γ extremum.⁸ The fact that the inelastic contribution represents more than 50% of the total conductance above 30 mV is a clear evidence for specular tunneling. Although the two larger structures already show up at 9.6 kbar (~2%), their amplitude again increases sharply between 12 and 13 kbar and saturates at more than 20% for pressure higher than 13 kbar.

We are not aware of experimental determination concerning the zone-edge phonons of GaSb in the literature. A simple scaling, however, which uses GaAs data¹⁴ and the main peaks of the GaSb phonon density of states¹⁵ allows a tentative indexing. Neglecting the small pressure dependence of the phonon energies, we find that the two first structures unambiguously correspond to the TA(111) and LA(111) phonons. The third at 26 meV is most likely due to the TO(111) one. The fourth peak at 30.2 meV shown in Fig. 3 cannot be fitted with a (111) phonon. Therefore either no LO(111) structure appears or it is buried in the other peaks.

We are unable to draw a firm conclusion about the symmetry of the fourth structure. Like the three first peaks, the fourth one also corresponds to a conductance increase at forward bias (3%). Returning to the $P=0$ curve locally magnified (Fig. 3), we observe that a small structure is present around the same bias voltage. Its line shape, which is neither totally even nor odd, can be described by two peaks and a dip. The second peak and the dip correspond fairly well to the LO(000)=29.8-meV and TO(000)=28.6-meV phonon energies determined by lattice reflection¹⁵ at 4.2°K. This type of structure has been generally attributed to self-energy effects although recently it has been proposed that real phonon emission should also contribute¹⁷ to the line shape. Our results at high pressure support this proposal since $\mu_F(111)$ is lower than the two above phonon energies, and no self-energy effect is therefore expected to occur for $V > 0$. The fourth structure at high pressure corresponds roughly to the second peak of the $P=0$

line shape so that we tentatively assign it to the LO(000) phonon. We have detected two other structures at higher biases corresponding to the LO(000)+LA(111) and LO(000)+TO(111) energies following the indexing of Fig. 3. This fact supports the idea that the 30.2-meV structure cannot be attributed to a (111) band-edge phonon.

In summary, we have discussed three essential features of tunneling: the background resistance, the inelastic processes, and the resistance kink. Their behavior consistently suggest that the total emptying of the Γ minimum occurs around $P_1 = 13$ kbar. Since the interband pressure coefficient has also been determined, we conclude that the crossover of the two bands occurs at $P_0 = 11$ kbar instead of 8 kbar as expected from the literature. A similar extrapolation leads to a room-pressure band separation of 110 meV instead of the reported 80 meV.⁵ Whether the high level of the doping and band tailing might be responsible for these discrepancies is unclear at the present time. As a conclusion, it is worth mentioning that the sharpness and the consistency of the observed phenomena allow a reliable and quantitative study of the relationship existing between band structure and tunneling.

We wish to thank D. Jerome for making available the high-pressure apparatus of Orsay, and E. Guyon for helpful discussions. Grateful acknowledgments are also due to A. Gousskov of the Faculté des Sciences of Montpellier who was kind enough to pull the GaSb ingot for us.

*Work supported by the Délégation Générale à la Recherche Scientifique et Technique.

¹C. B. Duke, *Tunneling in Solids* (Academic, New York, 1969), pp. 54–57.

²L. Esaki and P. J. Stiles, *Phys. Rev. Lett.* **16**, 574 (1966).

³J. J. Hauser and L. R. Testardi, *Phys. Rev. Lett.* **20**, 12 (1968).

⁴J. R. Vainsys, D. B. McWhan, and J. M. Rowell, *J. Appl. Phys.* **40**, 2623 (1969).

⁵E. H. Van Togerloo and J. C. Wooley, *Can. J. Phys.* **47**, 241 (1969).

⁶D. G. Seiler and W. M. Becker, *Phys. Rev.* **186**, 784 (1969).

⁷J. W. Conley and G. D. Mahan, *Phys. Rev.* **161**, 681 (1967).

⁸L. C. Davis and F. Steinrisser, *Phys. Rev. B* **1**, 614 (1970).

⁹J. W. Conley and J. J. Tiemann, *J. Appl. Phys.* **38**, 2880 (1967).

¹⁰G. Malfait and D. Jerome, *Rev. Phys. Appl.* **4**, 467

(1969).

¹¹P. Guétin and G. Schröder, to be published.¹²Precise determination of the barrier height in similar experimental conditions and quantitative estimation of the differential resistance shape will be the subject of a future publication.¹³The $P=0$ curve was drawn from a slightly more re-

sistive sample which was not studied under pressure.

¹⁴G. Dolling and R. A. Cowley, Proc. Phys. Soc., London 88, 463 (1966).¹⁵S. S. Mitra, Phys. Rev. 132, 986 (1963).¹⁶M. Hass and B. N. Hennis, J. Phys. Chem. Solids 23, 1099 (1962).¹⁷L. C. Davis, Phys. Rev. B 2, 4943 (1970).

Exact Solutions of the Self-Induced Transparency Equations

R. K. Bullough and F. Ahmad

Department of Mathematics, University of Manchester Institute of
Science and Technology, Manchester 1, England

(Received 28 December 1970)

We report exact solutions of the equations of self-induced transparency which generalize the linear theory of refractive index up to theoretical peak intensities of 10^{15} W cm⁻². The refractive indices are real, and there is no dissipation from inhomogeneous broadening. We solve the dielectric-surface problem for these solutions. We note the possibility of regaining previous analytical solutions in a fashion which permits a slight extension and some critical examination of these.

The semiclassical equations of motion for a single, undamped two-level atom exposed to a plane-polarized electromagnetic field \vec{E} of arbitrary strength can be expressed in the pseudo Bloch form

$$d\vec{r}/dt = \vec{\omega} \times \vec{r}; \quad \vec{\omega} = (\omega_1, 0, \omega_3). \quad (1)$$

We consider a uniform dielectric consisting of n such atoms per unit volume and no host atoms. The two-level atoms couple via the Maxwell wave equation

$$\nabla \times \nabla \times \vec{E} + c^{-2} \partial^2 \vec{E} / \partial t^2 = -4\pi n c^{-2} \partial^2 \vec{P} / \partial t^2, \quad (2)$$

where c is the velocity of light *in vacuo*. We report exact solutions of this system of equations which contain two free parameters, namely, a frequency or reciprocal temporal length v and the field amplitude E , and which are valid on or off atomic resonance.¹ We also report corresponding rotating solutions. The solutions are distortionless in the exact sense of this, rather than in the sense of Crisp² or of Arrechi *et al.*,³ i.e.,

$$\vec{E}(\vec{x}, t) = \vec{E}(\vec{x} - \vec{V}t), \quad (3)$$

and exhibit self-induced transparency (SIT) first reported by McCall and Hahn.^{4,5} They appear to be the natural nonlinear generalizations of linear theory and considerably extend our understanding of the SIT phenomenon. The mathematical theory bears directly on that of all the previous analytical SIT solutions.²⁻⁸

The notation in (1) is as follows: $\vec{r} = (r_1, r_2, r_3)$; $r_1 \equiv \rho_{s0} + \rho_{0s}$; $r_2 \equiv i(\rho_{s0} - \rho_{0s})$; and $r_3 \equiv \rho_{ss} - \rho_{00}$. The two atomic states are labeled s (upper) and 0 , and $\rho = \rho(\vec{x}, t)$ is the density operator. The atom's energy spacing is $\hbar\omega_s$ and $\omega_3 \equiv \omega_s$. The interaction is contained in

$$\omega_1 \equiv \omega_1(\vec{x}, t) \equiv -2ex_{0s} \hbar^{-1} E(\vec{x}, t); \quad (4)$$

$x_{0s} = x_{s0}$ is the matrix element of the dipole operator x . The atoms are inhomogeneously broadened: In (2),

$$\vec{P}(\vec{x}, t) = \hat{u} ex_{0s} \int_0^\infty g(\omega_s) r_1(\omega_s, \vec{x}, t) d\omega_s, \quad (5)$$

with $g(\omega_s)$ normalized to unity; \hat{u} is a unit polarization vector. Since the medium is isotropic, $\vec{E}(\vec{x}, t) = \hat{u}E(\vec{x}, t)$, and only the magnitudes $E(\vec{x}, t)$ and $P(\vec{x}, t)$ appear in the theory.

A "sharp-line" solution is one for which $g(\omega_s) = \delta(\omega_s - \omega_0)$. An important result is that if we can find a sharp-line solution of (1) and (2) which is valid on or off resonance, we can always find an inhomogeneous